

预混天然气小尺度燃烧特性的 CFD 研究

许 考, 刘中良, 康天放, 马重芳

(北京工业大学 环境与能源工程学院 教育部传热强化与过程节能
重点实验室和北京市传热与能源利用重点实验室, 北京 100022)

摘 要: 运用计算流体力学(CFD)二维模型研究预混天然气在小尺度空间内燃烧及墙壁的导热系数、外部的热损对燃烧特性的影响。研究表明, 墙壁的导热系数和外壁面的热损直接影响着火焰的点燃、稳定及氮氧化物的生成。对于预混气体, 仅存在一个很小的流区能维持通道内的燃烧。最后分析了轴向及径向的温度梯度对燃烧器的影响, 找到了在模拟条件下最佳的热力条件, 并以此达到优化小尺寸燃烧器的目的。

关 键 词: 天然气; 小尺度燃烧; 燃烧特性; 导热

中图分类号: TK124 文献标识码: A

1 引 言

作为一种轻型能源供应设备, 由于燃烧工质碳氢化合物具有较高的热值, 小尺寸燃烧器将逐渐取代对环境非友好、价格昂贵的锂电池^[1]。此外, 由于小尺寸燃烧系统有较高的传热系数, 因此可以降低燃烧体系的温度, 从而适当降低体系内热力型氮氧化物的生成。

目前, 在小尺度燃烧器设计方面遇到最大的挑战是如何在维持体系正常燃烧与热输出功最大化之间保持最佳的平衡状态^[2]。例如: 燃烧器尺寸减小到 1%, 其表面积和体积减少 4 和 6 个数量级, 比表面积增加 100 倍。比表面的增加必然使得体系热损增加, 从而影响燃烧器的稳定燃烧, 甚至有可能抑制体系的点燃或使得燃烧反应结束; 另一方面, 燃烧的输出功取决于系统的温度和比表面, 比表面越大, 对

输出功越有利, 而温度的增加又使得燃烧过程中热力型氮氧化物增加。目前对于小尺寸燃烧器的研究, 主要集中在燃烧火焰的稳定性方面^[3-5], 而如何使燃烧产生较高的效率, 同时对减少氮氧化物排放的报道仍然很少。由于燃烧体系的尺寸较小, 很难通过实验研究来验证, 因此数值成为理想的、可行的方法来研究小尺寸燃烧器燃烧特性, 并从理论上进行系统优化设计。

本文运用计算流体力学(CFD)二维椭圆模型研究预混天然气在小尺度空间内燃烧及墙壁的热力条件对燃烧特性的影响, 并从理论上提出了如何优化小尺寸燃烧系统, 使得既能稳定燃烧, 又能充分利用热能和减少氮氧化物排放的目的。

2 数值模型

2.1 模型类型及网格划分

天然气和空气经过预混进入小尺寸燃烧器, 该小尺寸燃烧器直径为 1.2 mm, 壁厚 50 μm , 长度 12 mm。由于该燃烧空间为轴对称的, 故选取二维轴对称截面作为模拟区域, 网格划分为非均匀的, 在燃烧区密度较大(见图 1), 并用有限体积法离散二维连续、动量、组分方程及二维固体导热方程, 运用 Fluent 6.1(Fluent 2002)对小尺寸燃烧空间进行数值模拟, 试图更加清晰地理解该燃烧区域内产物的浓度与温度的分布情况, 以此来理解燃烧规律及建立有效的理论模型。

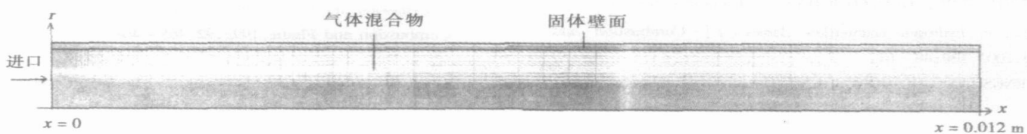


图 1 二维轴对称网格划分示意图

收稿日期: 2005-03-28; 修订日期: 2005-06-22

基金项目: 北京市传热与能源利用重点实验室开放基金资助项目(05005790200406)

作者简介: 许 考(1978-), 男, 江苏泗洪人, 北京工业大学博士研究生。

在模拟计算中,混合气体密度由不可压缩理想气体定律求得,混合气体的动力粘性系数、比热及导热系数由各个组分性能参数加权平均得到,混合气体中各个组分的比热表示为温度的函数。基于甲烷均相燃烧反应机理,其一阶不可逆反应速率表达式为^[9]:

$$R_{\text{CH}_4} = 2.119 \times 10^{11} \exp\left[\frac{-2.027 \times 10^8}{RT}\right] \times [\text{CH}_4]^{0.2} [\text{O}_2]^{1.3} \quad (1)$$

式中:

R —通用气体常数, $\text{J}/(\text{kmol} \cdot \text{K})$;

R_{CH_4} —甲烷的化学反应速率, $\text{kmol}/(\text{m}^3 \cdot \text{s})$;

$[\text{CH}_4]^{0.2} [\text{O}_2]^{1.3}$ —反应物浓度函数表达式。

边界条件如表 1 所示,其中进口混合气体以稳定的速度进入,层流态流动(雷诺数 $Re < 10$)。为了在出口处有更好的收敛速度,使用压力出口类型来定义出口处的静压。在墙壁和流体的交界面处,忽略了径向的扩散通量。交界面处的热流量由傅立叶导热定律和对流换热表达式共同决定。假定墙壁的左右两个面为绝热面,墙壁的导热系数和墙壁外部的热流密度作为独立的参数来研究体系内的燃烧特性。

表 1 燃烧室边界条件

| | 参数值 |
|--|-------|
| 进口速度(轴向) $/\text{m} \cdot \text{s}^{-1}$ | 0.5 |
| 进口甲烷质量分数 | 0.052 |
| 进口氧气质量分数 | 0.21 |
| 进气温度 $/\text{K}$ | 300 |
| 燃烧室直径 $/\text{mm}$ | 1.2 |
| 燃烧室壁厚 $/\text{mm}$ | 50 |

2.2 模型方程

燃烧体系内混合气体为层流流动,描述该流动状态的方程有质量守恒、动量守恒、组分及能量守恒,结合甲烷一阶均相化学反应(见式(1)),其二维稳态轴对称方程简化为:

连续方程:

$$\frac{\partial}{\partial x}(\rho u) + \frac{1}{r} \frac{\partial(r\rho v)}{\partial r} = 0 \quad (2)$$

动量方程:

$$\frac{\partial}{\partial x}(\rho uu) + \frac{1}{r} \frac{\partial}{\partial r}(r\rho uv) = -\frac{\partial p}{\partial x} + \frac{\partial}{\partial x}\left(\mu \frac{\partial u}{\partial x}\right) + \frac{1}{r} \frac{\partial}{\partial r}\left(r\mu \frac{\partial u}{\partial r}\right) \quad (3)$$

$$\frac{\partial}{\partial x}(\rho uv) + \frac{1}{r} \frac{\partial}{\partial r}(r\rho vv) = -\frac{\partial p}{\partial r} + \frac{\partial}{\partial x}\left(\mu \frac{\partial v}{\partial x}\right) + \frac{1}{r} \frac{\partial}{\partial r}\left(r\mu \frac{\partial v}{\partial r}\right) \quad (4)$$

组分方程:

$$\frac{\partial}{\partial x}(\rho u y_i) + \frac{1}{r} \frac{\partial}{\partial r}(r\rho v y_i) = \frac{\partial}{\partial x}(\rho D_{i,m} \frac{\partial y_i}{\partial x}) + \frac{1}{r} \frac{\partial}{\partial r}(r\rho D_{i,m} \frac{\partial y_i}{\partial r}) + R_i M_i \quad (5)$$

混合气体的能量方程:

$$\frac{\partial}{\partial x}(\rho hu) + \frac{1}{r} \frac{\partial}{\partial r}(r\rho hv) = \frac{\partial}{\partial x}\left(\lambda_f \frac{\partial T}{\partial x}\right) + \frac{1}{r} \frac{\partial}{\partial r}\left(r\lambda_f \frac{\partial T}{\partial r}\right) + \sum_i \left[\frac{\partial}{\partial x}(h_i \rho D_{i,m} \frac{\partial y_i}{\partial x}) + \frac{1}{r} \frac{\partial}{\partial r}(r h_i \rho D_{i,m} \frac{\partial y_i}{\partial r}) \right] - \sum_i h_i M_i R_i \quad (6)$$

固体能量方程:

$$\frac{\partial}{\partial x}\left(k_w \frac{\partial T}{\partial x}\right) + \frac{1}{r} \frac{\partial}{\partial r}\left(rk_w \frac{\partial T}{\partial r}\right) = 0 \quad (7)$$

其中:

M_i —组分的摩尔质量, kg/kmol ;

$\lambda_f = 995.6 + 0.096 T$, $\text{J}/(\text{kg} \cdot \text{K})$ (图 1~图 5 中);

$k_w = 1.692 - 0.00193 T + 3.196 \times 10^6 T^2$;

$\mu = \sum_i \mu_i y_i$; $\lambda_f = \sum_i \lambda_i y_i$;

$$D_{AB} = 1.858 \times 10^{-3} T^{3/2} \frac{(1/M_A + 1/M_B)^{1/2}}{p \sigma_{AB}^2 \Omega_D}$$

3 模拟结果及分析

3.1 小尺度燃烧特性

为了取得理想的模拟结果,网格划分时采用变节点划分方法,将模拟区域分别划分成 25 546(图 2 下部虚线表示)、20 000(图 2 中间用点表示)和 13 455 个(图 2 上部线条表示)节点。由图 2 可以发现,当网格节点数为 13 455 时,轴线上温度分布图并不能明显发现起燃点;当网格节点数增加到 20 000 甚至稍大的时候,模拟结果明显发现起燃点(屈折点)在温度 1 100 K 附近。同时在相同条件的蜂窝陶瓷载体中测得的轴线温度见图 2,对比可以发现当节点为 20 000 时,图形基本与之相似(尽管温度值有差别,其是由于保温不够理想及陶瓷载体高温时产生辐射而造成的)。另外,模拟还发现当网格节点超过 25 546 时,模拟结果失真,与实测结果对比,并没有出现温度最高的火焰部分。因此,在以下的模拟中将网格节点划分为 20 000 较为合理。

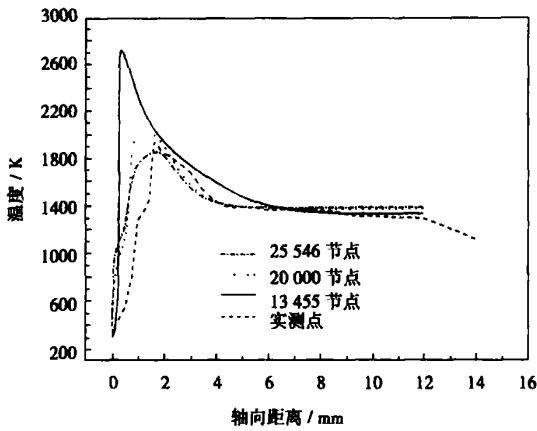


图 2 不同节点网络划分时轴线温度分布

图 3 为模拟区域温度、甲烷燃烧反应速率及甲烷浓度分布轮廓图。图 4 表示反应区内温度、反应速率沿着轴线和内壁面的分布图。结合图 3 和图 4 可以发现，燃烧区域内明显可以分成 3 个区，即预热区、燃烧区和冷却区(图 4 中的 1、2、3)。

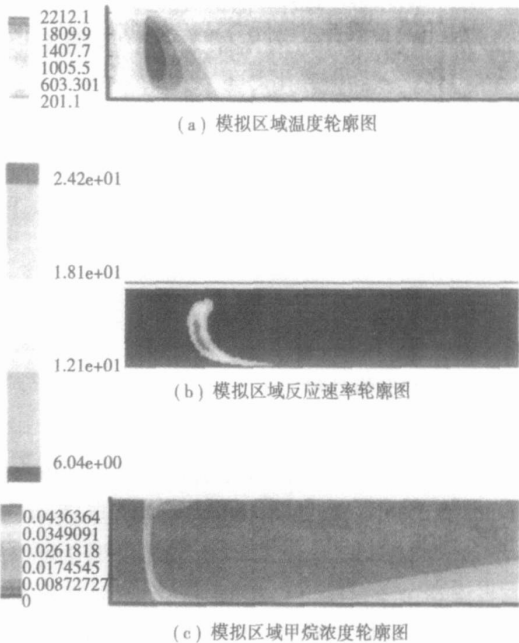


图 3 模拟区域温度、甲烷燃烧反应速率及甲烷浓度分布轮廓图

在预热区 1(见图 4)，内壁面温度明显显著高于混合气体温度，此时主要靠对流换热将能量传输给混合气体，同时下游壁面不断地通过热传导将热传给上游(预热区)壁面，一旦将壁面处的混合气体加热到燃点，被点燃后向中心传播直到稳定燃烧。由图 4 还可以发现，沿着壁面的反应速率④远远小于

轴线处燃烧区的反应速率③，上述模拟结果与文献 [3] 相一致。

当混合气体温度达到可燃温度 1 100 K 左右时，轴向温度分布图上明显出现了屈折点，以此点为分界点，混合气体开始迅速燃烧并释放大量的热，由于混合气体的传热比燃烧释放的热量要小得多，因此图 4 中温度曲线①出现了温度的峰值，即燃烧区。由于在燃烧区反应异常剧烈，基本上将反应物燃烧殆尽(见图 3(c))，此时进入冷却区。由于燃烧后的烟气不断与内壁面换热，最终烟气的温度和壁面温度趋于一致(见图 4)。

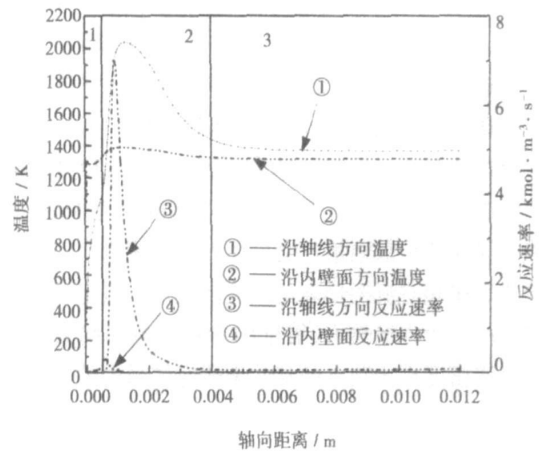


图 4 温度、反应速率沿着轴线和内壁面的分布

图 5(a)为外壁面为绝热的情况下燃烧体系内 NO_x 分布图。NO_x 生成采用 Leeds 大学发展的速率模型^[6]。由图 5 明显可以看出，在绝热条件下燃烧区 NO_x 浓度大约在 2.6E-5 左右，而在壁面有热损的条件下，浓度大约在 2.2E-5。此区域氮氧化物的产生主要由于高温引起的高温型氮氧化物^[7-8]。而实验发现，在近似绝热条件下，蜂窝陶瓷燃烧出口处检测到 NO_x 浓度为 2.4 ~ 2.5E-5，与模拟结果近似一致。

3.2 固体导热及外壁面热损对燃烧的影响

燃烧室壁的导热性能对小尺寸燃烧器的稳定运行起重要作用。一方面将后燃烧区的热量传给上游预热混合气；另一方面通过外部热损影响内部燃烧，延缓点燃或使得燃烧熄灭，同时也可以适当降低燃烧体系内热力型氮氧化物的生成。一旦燃烧体系内温度较高，不仅 NO_x 排放量增加，而且由于热应力作用使得燃烧室壁面变形破坏，甚至烧结。

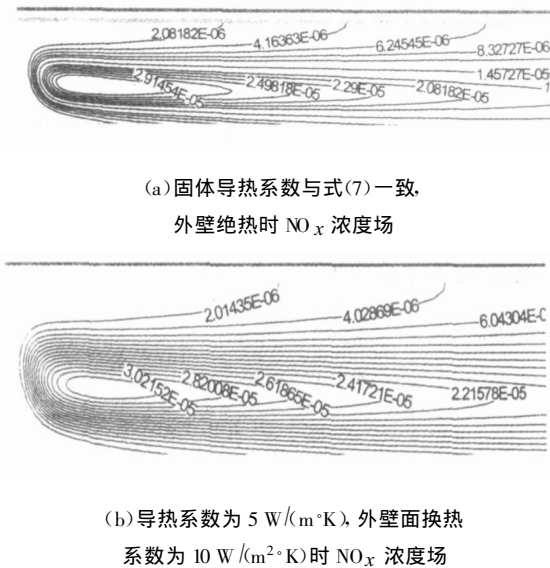


图 5 不同外壁面条件时,体系内 NO_x 浓度场

图 6 为外壁换热系数为 10 W/(m²·K), 不同墙壁导热系数时, 内壁面温度分布。由该图可以发现, 当燃烧室墙壁导热系数较小时, 在外壁面换热系数一定的情况下, 内壁面的轴向温度梯度很大; 当墙壁导热系数适中时, 内壁面的轴向温度分布较为均匀, 温度梯度较小; 当墙壁导热系数较大(超过 10 W/(m·K))时, 模拟中发现火焰熄灭。因此, 适当的导热系数对燃烧有利。

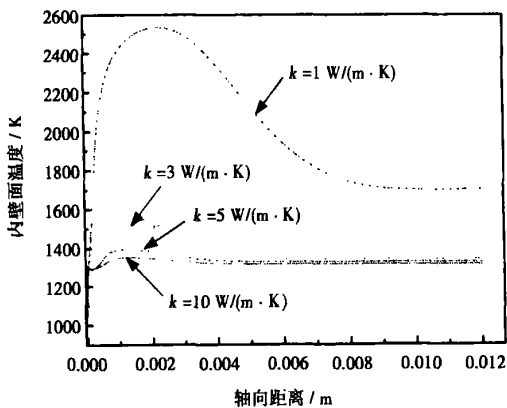


图 6 外壁换热系数为 10 W/(m²·K) 不同的墙壁导热系数时, 内壁面温度分布

图 7 为墙壁导热系数为 5 W/(m·K), 外壁面不同换热系数时, 径向温度梯度分布图。由该图可以发现, 在墙壁导热系数适中的情况下, 外部换热系数较小时, 径向温度梯度较小。反之, 径向温度梯度较大, 甚至导致燃烧熄灭。

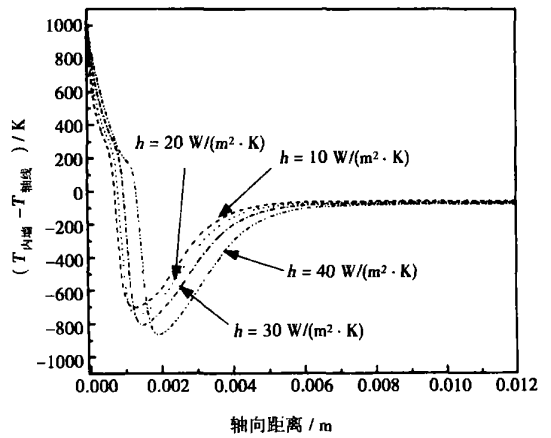


图 7 墙壁导热系数为 5 W/(m·K), 外壁面不同换热系数时径向温度梯度分布

因此, 根据模拟所设置的条件, 选择墙壁导热系数为 5 W/(m·K), 外壁面换热系数 10 W/(m²·K) 时, 对该燃烧系统较为有利。

图 5(b)即为墙壁导热系数为 5 W/(m·K), 外壁面换热系数 10 W/(m²·K) 时燃烧体系内 NO_x 分布图。对比(a)和(b)即发现, (b)中 NO_x 产物浓度比(a)平均低 2-3E-6。

3.3 混合气体的进口速度对燃烧的影响

图 8 表示在绝热的条件下着火点位置与混气进口速度之间关系。由图中可以看出, 当混气进口速度小于 0.4 m/s 时很难点燃(模拟 0.2 m/s 时, 无法点燃), 当混气以 0.5 m/s 时着火点位置距离进口最小, 随后随着进口速度增加, 距离不断增加, 当混气进口速度大于 2 m/s 时无法点燃。

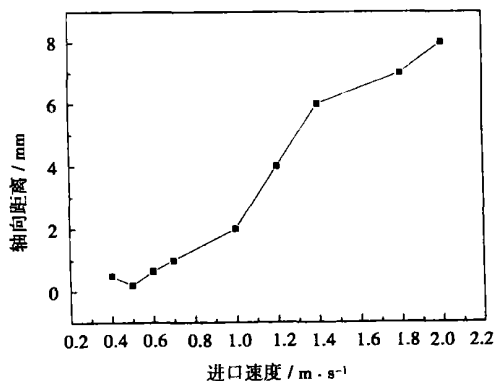


图 8 混气进口速度与点燃位置关系

由传热学分析可知, 当混合气体进入小尺度燃

烧器内,首先与壁面进行换热使温度升高到燃点方可被点燃。当混合气体以较快速度进入时候,由于没有充分的时间和壁面进行换热,很难将其加热至燃点。对于混合气体以很低的流速进入小尺寸燃烧器时候,由于进口附近壁面一直保持很高的温度,同时反应区因燃烧产生的热量减少,结果与产生的热量相比,热损增加了许多,最后使得燃烧无法进行。

4 结 论

通过对小尺寸燃烧体系模拟及结果分析,可以得出以下结论:

燃烧体系的固体导热系数和外壁面的热损对体系内燃烧的正常进行起重要作用。在外壁面热损一定的条件下,如果墙壁导热系数越小,会使得内壁面的温度梯度剧增,在热应力的作用下很容易使得燃烧壁面变形或烧结,同时 NO_x 的排放增加;越大,由于与外界产生热交换而热损增加使得无法点燃。对于固体导热系数一定的条件下,外壁面热损越大,径向的温度梯度越大,热损越大,从而使得无法点燃,越小,燃烧体系温度增加。只有在适当的热力条件下(本模拟中导热系数为 $5 \text{ W}/(\text{m} \cdot \text{K})$ 和换热系数为 $10 \text{ W}/(\text{m}^2 \cdot \text{K})$),燃烧体系才能在高效、稳定和环保节能的工况下运行。

其次,在绝热的条件下,要选择适当的混合气体

进口速度,方能保证燃烧体系的正常运行。

参考文献:

- [1] 钟北京,洪泽恺.微燃烧器内甲烷催化燃烧的数值模拟[J].热能动力工程,2003,18(6):584-587.
- [2] YANG W M, CHOU S K, SHU C, *et al.* Microscale combustion research for application to micro Thermophoto-voltaic systems[J]. **Energy Conversion and Management** 2003, 44:2625-2634.
- [3] NORTON D G, VLACHOS D G. Combustion characteristics and flame stability at the microscale: a CFD study of premixed methane/air mixture[J]. **Chemical Engineering Science** 2003, 58:4871-4882.
- [4] FALCITELLI M, PASINI S, TONGNOTTI L. Modeling practical combustion systems and predicting NO_x emissions with an integrated CFD based approach[J]. **Computers and Chemical Engineering**, 2002, 26:1171-1183.
- [5] DAOU J. Influence of conductive heat loss on propagation of premixed fame in channels[J]. **Combustion and Flame** 2002, 128:321-339.
- [6] FLUENT COMPANY. Fluent 6.1. 18[M]. America: Fluent Company, 2002.
- [7] FRAZIERT R. Fuel/air mixing and NO_x formation in a clean premixed gas turbine combustion[D]. Urbana-Champaign: University of Illinois, 2000.
- [8] FALCITELLI M, PASINI S, TONGNOTTI L. Modelling, practical combustion systems and predicting NO_x emissions with an integrated CFD based approach[J]. **Computers and Chemical Engineering**, 2002, 26:1171-1183.

(何静芳 编辑)

新 机 组

1 800 kW 额定功率和 38%效率的回热式船用燃气轮机

据《Gas Turbine World》2005年7~8月号报道,法国 Turbomeca 正在研制 2 MW 级回热式燃气轮机,匹配到直接传动的直流发电机,用于船舶电力生产和推进系统,还用于铁路机车驱动电力牵引电动机。

回热式燃气轮机的额定输出功率为 1 800 kW,热效率为 38%。发动机设计是简单的,单轴转子有一个先进技术的离心压气机轮盘,其压比为 7.9:1,空气质量流量为 9 kg/s 。

燃烧室是顶部安装的单管逆流式设计,目前选择液体燃料运行。燃烧室设计使能在现场完成燃烧室的拆卸,并易于接近对位于顶部的喷射系统进行维护。

压气机由在同一根轴上的二级轴流涡轮驱动,在冷端输出驱动情况下轴的最大连续转速为 $22\,500 \text{ r/min}$ 。

转子轴的长度约为 910 mm,由轴向间隔(中心到中心)约 740 mm 的两个轴承支承,前轴承是滚珠轴承,后轴承是滚柱轴承(热端)。

(吉桂明 供稿)

利用 CCD 测量炉膛温度场及 NO_x 排放特性试验研究 = **Experimental Study of the Measurement of Furnace Temperature Fields and NO_x Emission Characteristics with the Help of a Charge-coupled Device (CCD)** [刊, 汉] / GUO Jian-min, LIU Shi, JIANG Fan, et al (Institute of Thermophysics under the Chinese Academy of Sciences, Beijing, China, Post Code: 100080) // Journal of Engineering for Thermal Energy & Power. — 2006, 21(1). — 39 ~ 42

Local high temperature in a furnace flame is a major cause leading to an increase in NO_x emissions. Furnace temperatures were measured by using a charge-coupled device (CCD) based pick-up camera with the temperature measurement principle pertaining to a dual-color method. Under various operating conditions an experimental investigation was conducted of the relationship between such factors as boiler load, excess air factor, coal rank, furnace temperature, burner operating mode, etc on the one hand and NO_x emission characteristics on the other. The results of the investigation indicate that with the change in various influencing factors the furnace temperature will undergo corresponding changes and the NO_x emissions also follow different variation laws. The charge-coupled device can effectively monitor the furnace temperature on a real-time basis and diagnose local high temperatures, thus resulting in an improved combustion and a better regulation of operating conditions as well as an effective lessening of NO_x emissions. **Key words:** charge-coupled device, NO_x , boiler

CO_2 稀释燃料对富氧扩散燃烧中 NO_x 生成的抑制作用 = **The Role Played by CO_2 Diluted Fuel in Suppressing NO_x Formation During an Oxygen-enriched Diffusion Combustion Process** [刊, 汉] / YANG Hao-lin (Department of Thermal Sciences & Energy Engineering, China National University of Science & Technology, Hefei, Anhui Province, China, Post Code: 230027), ZHAO Dai-qing, LU Guan-jun (Guangzhou Institute of Energy Conversion under the Chinese Academy of Sciences, Guangzhou, China, Post Code: 510604) // Journal of Engineering for Thermal Energy & Power. — 2006, 21(1). — 43 ~ 47

The reduction of NO_x emissions in a high-temperature flame is a key factor for furthering the widespread use of oxygen enriched combustion as a new type of energy-saving combustion technology. Based on the theory of NO_x suppression realized through the use of flue-gas recirculation, etc and with a counterflow diffusion flame serving as an object of investigation the impact on flame characteristics and NO_x formation by CO_2 diluted fuel under various concentrations of enriched oxygen was studied using a model of detailed elementary-reaction dynamics. The results of the study indicate that the impact of the CO_2 diluted fuel on combustion characteristics will tend to be conspicuous with an increase in oxygen concentration in an oxidation agent. Moreover, under a relatively high oxygen concentration the CO_2 diluted fuel can, in addition to maintaining a relatively high flame temperature, effectively reduce NO_x formation and NO_x emission index ELNO.

Key words: oxygen enriched combustion, fuel dilution, NO_x , numerical analysis

预混天然气小尺度燃烧特性的 CFD 研究 = **A CFD (Computational Fluid Dynamics) Study of the Small-scale Combustion Characteristics of Premixed Natural Gas** [刊, 汉] / XU Kao, LIU Zhong-liang, KANG Tian-fang, et al (Education Ministry Key Laboratory of Heat Transfer Intensification & Energy Conservation under the Institute of Environmental and Energy Engineering of the Beijing Polytechnic University, Beijing, China, Post Code: 100022) // Journal of Engineering for Thermal Energy & Power. — 2006, 21(1). — 48 ~ 52

A CFD (computational fluid dynamics) two-dimensional model was employed to study the combustion of premixed natural gas in a small-scale space and the impact of wall heat-conductivity factor and outer wall heat loss on the combustion characteristics. The results of the study indicate that the wall heat conductivity factor and the outer-wall heat loss have a direct influence on the ignition and stability of the flame and the formation of NO_x . As for the premixed natural gas there exists only a zone of very small flow velocity, which can maintain combustion in a channel. Finally, the impact of axial and radial temperature gradient on a combustor was analyzed and, an optimum thermodynamic condition under simulated circumstances has been identified, thereby making it possible to achieve the aim of optimizing a small-sized combustor.

Key words: natural gas, small-scale combustion, combustion characteristics, heat conduction

飞灰回燃对燃烧福建无烟煤 CFB 锅炉运行影响的研究 = **An Investigation of the Impact of Fly-ash Reburning on the Operation of an Anthracite-firing CFB (Circulating Fluidized Bed) Boiler** [刊, 汉] / HE Hong-zhou (Institute of Energy and Power Engineering under the Jimei University, Xiamen, China, Post Code: 361021) // Journal of Engineering for Thermal Energy & Power. — 2006, 21(1). — 53 ~ 57

The reactivity of fly-ash carbon and that of other coals fed into a boiler was investigated and compared through experiments with the help of a thermobalance. A theoretical analysis was conducted of the impact of fly-ash reburning on the combustion efficiency of a CFB (circulating fluidized bed) boiler. Moreover, by way of industrial tests investigated and measured was the impact of the fly-ash quantity recycled for reburning on the following items: the operating temperature of a recycle-to-boiler device, fly-ash particle distribution and its carbon content, boiler combustion efficiency and other operating parameters. The results of the investigation indicate that the reactivity of fly-ash carbon of the CFB boiler burning Fujian anthracite is higher than that of other corresponding coals fed into the boiler. In addition, other parameters, such as carbon content of the reburnt fly ash, the ratio of the reburnt fly ash amount to other coals fed into the boiler, have a major influence on the combustion efficiency of the boiler. The use of fly-ash reburning technology will be conducive to reducing the carbon content of the fly ash and the operating temperature of recycle-for reburning device as well as enhancing the combustion efficiency of the boiler. However, a relatively large amount of fly ash assigned for reburning will affect the stable operation of the boiler. **Key words:** Fujian anthracite, circulating fluidized bed boiler, fly ash, reburning

燃煤飞灰伏安特性的实验研究 = **Experimental Study of the Volt-ampere Characteristics of Fly Ash Resulting from Coal Firing** [刊, 汉] / YUAN Yong-tao, QI Li-qiang (Institute of Environmental Science & Engineering under the North China University of Electric Power, Baoding, China, Post Code: 071003) // Journal of Engineering for Thermal Energy & Power. — 2006, 21(1). — 58 ~ 61

The dielectric character of fly ash is a major factor having an impact on the efficiency of electrostatic precipitators. By employing a self-developed direct-current high voltage test system the current leakage and specific resistance of the fly ash of various kinds of coal being fired were measured and analyzed, and a series of volt-ampere characteristic curves obtained. It has been found that the relation among the following three items, i. e., the voltage applied to the ash layer, the current leakage through the ash layer and fly-ash specific resistance, does not always conform to the classic Ohm's law, namely, $V/I \neq \text{constant}$. At the three segments of high, middle and low voltage the volt-ampere characteristic curves of the fly ash have different configuration features. With an increase in voltage the specific resistance of the fly ash assumes a descending tendency with the range of descending amount being within one order of magnitude ($10^1 \Omega \cdot \text{cm}$). The cause leading to the occurrence of this phenomenon consists in the high-resistance feature of the fly ash. Meanwhile, this is also closely related with the physical-chemical properties of the coal rank and fly ash. **Key words:** fly ash of coal fired, dielectric properties, specific resistance, electrostatic precipitator

考虑两相流音速时气固两相流激波研究 = **A Study of Two-phase Shock Waves with a Two-phase Flow Sonic Velocity being Taken into Account** [刊, 汉] / ZHAO Liang-ju, GAO Li-juan, YUAN Yue-xiang, et al (Institute of Power Engineering under the Chongqing University, Chongqing, China, Post Code: 400044) // Journal of Engineering for Thermal Energy & Power. — 2006, 21(1). — 62 ~ 65, 69

On the basis of a two-phase flow sonic velocity a gas-solid two-phase flow shock-wave model was set up, and calculations and analyses were performed. When compared with the calculation results of a shock wave model based on a single-phase flow sonic velocity it has been found that in the case of a relatively large gas-phase volume the sonic velocity difference as calculated by using the above two kinds of models is relatively small and the shock wave results for the two models are in good agreement. When the gas phase volume is relatively small, the sonic velocity value calculated through the use of the two-phase sonic velocity model is in better correspondence with the actual value, resulting in more rational shock wave re-